Discriminant function analysis of maxillary bone measurements for sex estimation in a Colombian population by using cone-beam computed tomography

Sergio Iván Tobón-Arroyave [1,2], Santiago Palacio-Gutiérrez [1], Sara Morales-Galeano [1], Clara Inés Saldarriaga-Naranjo [3], Carlos Alberto Tangarife-Villa[4]

[1] Oral and Maxillofacial Surgery Program, Faculty of Dentistry, University of Antioquia. Medellín, Colombia. [2] Laboratory of Immunodetection and Bioanalysis, Faculty of Dentistry, University of Antioquia. Medellín, Colombia. [3] Department of Radiology, CES University and RADEX 3D Specialized Radiology Center. Medellín, Colombia. [4] Department of Basic Sciences, National Faculty of Public Health, University of Antioquia. Medellín, Colombia

Corresponding author:
sergio.tobon@udea.edu.co

The authors declare that they have no conflict of interest.

KEYWORDS

Cone beam computed tomography,
Discriminant analysis,
Forensic anthropology,
Forensic dentistry,
Maxilla,
Sex determination

J Forensic Odontostomatol
2025. Apr;(43): 1-19:32
ISSN :2219-6749
DOI: doi.org/10.5281/zenodo.15044914

ABSTRACT

Sexual dimorphism is an important biological factor for sex estimation from skeletal remains in medicolegal identification. This study aimed to determine using a discriminant function analysis, whether specific maxillary linear and angular measurements performed in cone-beam computed tomography (CBCT) images may be useful to determine the sex in a Colombian population. The sample consisted of 212 CBCT scans acquired from 86 males and 126 females. The protocol included the assessment of 23 parameters, of which 16 were bilateral and seven were non-bilateral. An intra-observer variability test was performed to ensure data reliability and unpaired t tests were applied to determine between-group differences. Significant predictor variables were subjected to univariate and multivariate discriminant function analyses. A total of five non-bilateral and 14 bilateral measures were statistically significant. Univariate discriminant analyses produced a mean percentage of correct prediction after cross-validation ranging from 55.20% to 72.60% for non-bilateral and from 58.70% to 73.10% for bilateral maxillary variables. The association of variables in the multivariate models increased the percentages of correct sex prediction even after cross-validation up to 77.80% for non-bilateral and up to 77.40% for bilateral maxillary measurements. It was concluded that CBCT measurement of maxillary bone parameters may be applied as a complementary technique to discriminate the sex from human remains through discriminant function analysis methods in the Colombian population.

INTRODUCTION

Sexual dimorphism has been defined as the systematic difference in size, shape, or color among males and females of the same species.[1] Although this phenomenon in humans is lesser than in nonhuman primates, allows a great discrimination of the individuals according to its chromosomal sex.[2] In this line, it has been acknowledged that skeletal characteristics are determined by an individual genetic background, its environment, and the functional demand.[3] Due to hormone-dependent variations,[4] men have developed greater muscularity in comparison to women, which has led to a larger stature as well as more robust and demarcated cranial and facial traits.[5,6] Sex estimation from skeletal remains is a procedure that has been used in the identification process

during medico-legal examination of decomposed, fragmented, burned, or skeletonized bodies[2,6,7] as bones are considered one of the most stable tissues of the human being.[8] In parallel, craniometric analysis has demonstrated to be an outstanding method for anthropological examination, given its objectivity, reproducibility and statistical value,[9] though its applicability for determining the sex of a cranium is only feasible in adults, when the development of secondary sexual characteristics has been completed.[10] Under this perspective, while some researchers have demonstrated that a number of isolated cranial anatomical structures may be useful in the estimation of sex,[6,8,10] maxillary bone, a fundamental structure for the facial formation and stability, has shown to have many morphological variations and dimensional differences that might be strongly liaised to sex.[8,11-13]

Various techniques have been used in forensic sciences to assess the dimensions of anatomical structures in order to establish the sex of cranial skeletal remains including measurements on dry skulls, conventional radiography, computed tomography, and cone-beam computed tomography (CBCT).[7] Among these, convincing evidence has demonstrated the ability of CBCT images to characterize the morphology of different structures of the maxillary bone and to determine the variations in the morphometric characteristic with high-dimensional accuracy.[8,12-17] Nevertheless, research data in this field have been divergent and may differ according to the populations studied, the methodological approaches, and diagnostic tools used.

Additionally, anthropometric studies have used different statistical models for sex identification,[5] among which discriminant function analysis has been widely employed with excellent results.[6] This method uses linear combinations of quantitative variables to determine and predict group membership (i.e., male or female) within the sample, seeking the best combination that maximizes inter-class difference and minimizes intraclass variance. Even so, it has been described that discriminant functions are sensitive to population variations, so that these formulas should be locally settled and validated for individual populations considering the variations in ethnic parameters affecting the phenotypic characteristics.[6,10] Considering that maxillary bone dimensions have shown great inter- and intra-population variability,[13,18] this study aimed to determine using a discriminant function analysis, whether specific maxillary linear and angular measurements performed in CBCT images may be useful to determine the sex in a Colombian population.

MATERIALS AND METHODS

Study design, sample population, and setting:

This cross-sectional study was evaluated and approved by the Ethical Research Board (Approval N° 62-2020) and the Technical Research Council (Code 2021-40871) of the Faculty of Dentistry of the University of Antioquia. All aspects of the research were performed in compliance with the ethical standards outlined in the Declaration of Helsinki. The sample size was estimated based on the patients' population referred for CBCT imaging of the maxillary bone, during the period from June 2020 to December 2022, to a private imaging specialized center (RADEX 3D Specialized Radiology Center) in Medellín, Colombia. Taking into account a total of 467 referred patients, an online calculator tool (Raosoft® Inc., Seattle, WA, USA) indicated a sample size requirement of at least 212 digital imaging and communications of medicine (DICOM) files to identify significant between-group differences in the bivariate comparisons with a 95% confidence level and 5% margin of error. Eligible cases were those aged 18 years or older with no congenital, pathological, or traumatic lesions of the maxillary bone. Exclusion criteria applied were evidence of ongoing orthodontic treatment or maxillofacial surgery, limited field of view hampering the visualization or location of the maxillary landmarks, and poor quality of CBCT images. Written informed consent was obtained from each patient for the use the scans for research purposes prior to CBCT imaging and data were used anonymously.

All of the cases underwent CBCT scanning with an i-CAT® 17-19 system (Imaging Sciences International, Inc., Hatfield, Pennsylvania, USA) at 120 kVp, 37.07 mA, 16 cm x 13 cm of field vision, 0.20 mm voxel size, and acquisition time of 26.9 seconds. Both the Frankfort horizontal and the midfacial planes were used to construct the horizontal and vertical axes of the reference

frame during the scanning process to avoid measurement pitfalls induced by the head position. Using the i-CATVision 1.9® software (Imaging Sciences International), CBCT scans were examined synchronously by two experienced Maxillofacial Surgeons (S.P.-G. and S.M.-G.) calibrated by a single "gold-standard" Maxillofacial Radiologist (C.I.S.-N.). The calibration was accomplished using illustrative images and written descriptions of the morphometric features to be measured. Any discrepancy between raters was arbitrated by using the Maxillofacial Radiologist judgment. Measurements were conducted on a computer screen in a darkened room by using the maximum intensity projection mode of the software to reach superior image contrast and the magnification function to amplify the images.

Patient-related data acquisition

Before performing the measurements, study sample characteristics such as age of the patient at the time of CBCT acquisition and sex (i.e., male vs female) were documented for each CBCT included in the study. Likewise, the alveolar process status was documented separately for each maxillary segment (i.e., right posterior, left posterior, and anterior maxilla) and categorized based on the absence of teeth (Fig. 1a-f) as fully dentate or completely/partially edentulous (with totally edentulous maxillary segments or at least one extracted tooth, except third molars).[19]

Figure 1. Panoramic views of a panel of CBCT scans showing representative features of the alveolar process status in different maxillary segments. (a) Dentate anterior alveolar process showing the presence of the six anterior superior teeth. (b) Partially edentulous anterior alveolar process displaying the loss of both maxillary central incisors. (c) Completely edentulous maxillary alveolar process as defined by the loss of all anterosuperior teeth. (d) Dentate right posterior alveolar process containing the two premolars and molars (except the third molars) within the alveolar bone. (e) Partially edentulous posterior alveolar process illustrated by the loss of the second premolar and first molar teeth in the left maxillary side. (f) Completely edentulous left posterior maxillary alveolar process showing the total absence of teeth.

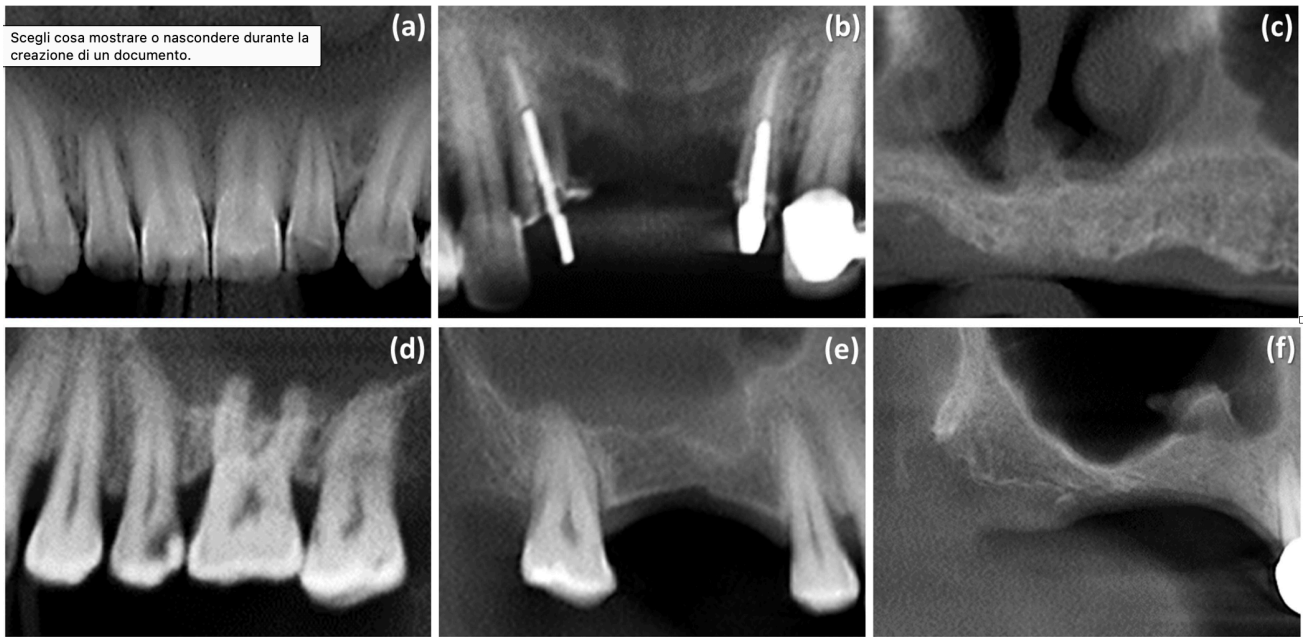

Landmarks selection for morphometric assessment

Using multiplanar reconstructions, the measurement protocol was composed of two sets of measurements. The first set included seven non-bilateral maxillary parameters and the second set of measurements was composed by 16 bilateral maxillary morphometric data. Linear measurements were obtained in millimeters (mm) using the distance measuring tool of i-CATVision® software, whereas angular measurements were taken in degrees (°) with the aid of an image analyzer system (AxioVision 3.1®, Carl Zeiss®, Oberkochen, Germany) as follows:

- Non-bilateral maxillary variables included the length of the maxillary complex, determined in

the axial plane viewing simultaneously a line drawn through the palatal plane in the sagittal image, as the greatest distance between tip of the anterior nasal spine (ANS) of the maxilla and the tip of the posterior nasal spine (PNS) of the palatal bone; as well as the maximum inter-maxillary width, measured as the greatest distance between the right and left maxilla taken between lateral walls of the two maxillary sinuses (MS) (Fig. 2a). Furthermore, in the sagittal plane, several morphometric parameters were measured on the maxillary midline according to earlier descriptions (Fig. 2b and c),[13,16,17] including: the nasopalatine canal (NPC) length, measured as the distance among the midpoints of incisive foramen (IF) and nasopalatine foramen (NPF); the NPC angle, located anteriorly among the axis of NPC and the palatal plane; the minimum anterosuperior buccal bone thickness, measured as the shortest distance from the NPC to the buccal cortical border; the anteroposterior width of IF, assessed at the level of the hard palate; and the anteroposterior width of NPF, assessed at the nasal fossae level. When the NPC had two or more nasal and/or palatal openings, all the anteroposterior widths of visible foramina were summed.

- Bilateral maxillary morphometric data included the measurement of maximum craniocaudal, anteroposterior, and transverse dimensions of the MS (Fig. 3a-c). The maximum craniocaudal dimension (height) of the MS was measured on coronal reconstructions as the distance between the most superior and inferior points, while the anteroposterior (depth) and transverse (width) dimensions were determined on axial sections measuring the distances between the most anterior and posterior walls and among the most lateral and medial points of the MS, respectively. Also, the minimum distance from the MS floor to the alveolar crest (AC) was estimated by tracing a perpendicular line from the deepest point of the MS floor within the alveolar process to the surface of the alveolar crest viewing simultaneously the panoramic and coronal images (Fig. 3d and e).[13] Furthermore, in the infraorbital region, the greater width of infraorbital foramen (IOF), measured in the anterior wall of MS in the three orthogonal planes, and the vertical distance from the IOF to the AC[20,21] were included in the analysis (Fig. 3f-h). Finally, the morphometric assessment of the greater palatine canal (GPC) included the length of the GPC in the sagittal plane, measured from the central point of the pterygopalatine fossa to the central point of the greater palatine foramen (GPF)[22] taking into account the sum of the length of two lines intersecting in the center of the canal (Fig. 3i); the maximum anteroposterior width of the GPC in the axial plane and its distance to the pterygoid hamulus, NPC, and posterior nasal spine (PNS)[15,23] measured with the sagittal palatal plane positioned through the center of the supero-inferior dimension of the hard palate (Fig. 3j); the distance from the medial wall of GPF to the midline maxillary suture (Fig. 3k)[15,24] the distance from the center of GPF opening to the AC (Fig. 3k); and the angle between the vertical axis of the GPC and the horizontal plane of the palatine bone measured in the coronal view (Fig. 3l).[11,15]

Data management and statistical analysis

All data were statistically analyzed using standard statistical software (SPSS, v.29.0, IBM, Armonk, NY). Immediately after a twelve-month study period, which focused on completing all of the required measurements, 10% of the sample (21 CBCT scans) selected following a simple random sampling procedure, was reassessed simultaneously by the same examiners and the intraclass correlation coefficient (ICC) was calculated to determine intra-observer variability. Interpretation of ICC was based on the following categorization system: values <0.40 indicated poor reproducibility, 0.40-0.59 indicated fair reproducibility, 0.60-0.74 good reproducibility, and values ≥0.75 indicated excellent reproducibility.[25]

The distribution pattern of quantitative variables was analyzed using the Kolmogorov-Smirnov (K-S) test. Considering that the data showed a normal distribution pattern (P-values ranging from 0.062 to 0.200, K-S test), they were analyzed using the parametric t-test for independent samples to identify differences between the sexes. Homoscedasticity was verified through Levene's test for equality of variances. Also, Pearson's chi-square test (χ^2) was used to compare categorical variables. All significant predictor variables identified in the bivariate analyses were subjected to univariate discriminant analyses to calculate the mean percentage of correct prediction after cross-

validation of each of them. Cross-validation was used to adjust for the percentage of misclassified observations.[10] Afterward, a multivariate discriminant function analysis was conducted using the variables that presented a mean correct prediction percentage above 60% to estimate the sexual dimorphism of the sample. Wilks' lambda (λ) and Box's M tests were used to examine the statistical significance of the discriminant functions and the homogeneity of covariance matrices, respectively. Furthermore, eigenvalues and canonical correlations were also included to analyze the relationships among predictor variables and the sex categories. Fisher's linear discriminant function coefficients of the selected variables, with their respective constants, yielded to the development of the following equation as previously suggested:[1,6,10] N = b1* x1 + b2 * x2 + bm * xm + a, where b1 through bm represent the discriminating coefficients, x1 through xm are discriminating variables, and a is the discriminant function constant. To assign the sex, the values of measurements must be separately substituted in the equation for male and female, so that the greater value of N indicates the sex.[6,10] The level of significance was set at 5% (α = 0.05).

Figure 2. CBCT images showing morphometric evaluations of different non-bilateral maxillary landmarks. All of the lines were heightened using the AxioVision® software to illustrate the path by which the measurements were performed: (a) Axial section displaying the measurement of *(1)* maxillary complex length (distance ANS-PNS) and *(2)* maximum inter-maxillary width. (b) Sagittal section showing the measurement of *(1)* length of the NPC, *(2)* width of NPF and *(3)* width of IF. (c) Sagittal section illustrating the assessment of *(1)* the minimum anterosuperior buccal bone thickness and *(2)* the NPC angle with reference to the palatal plane.

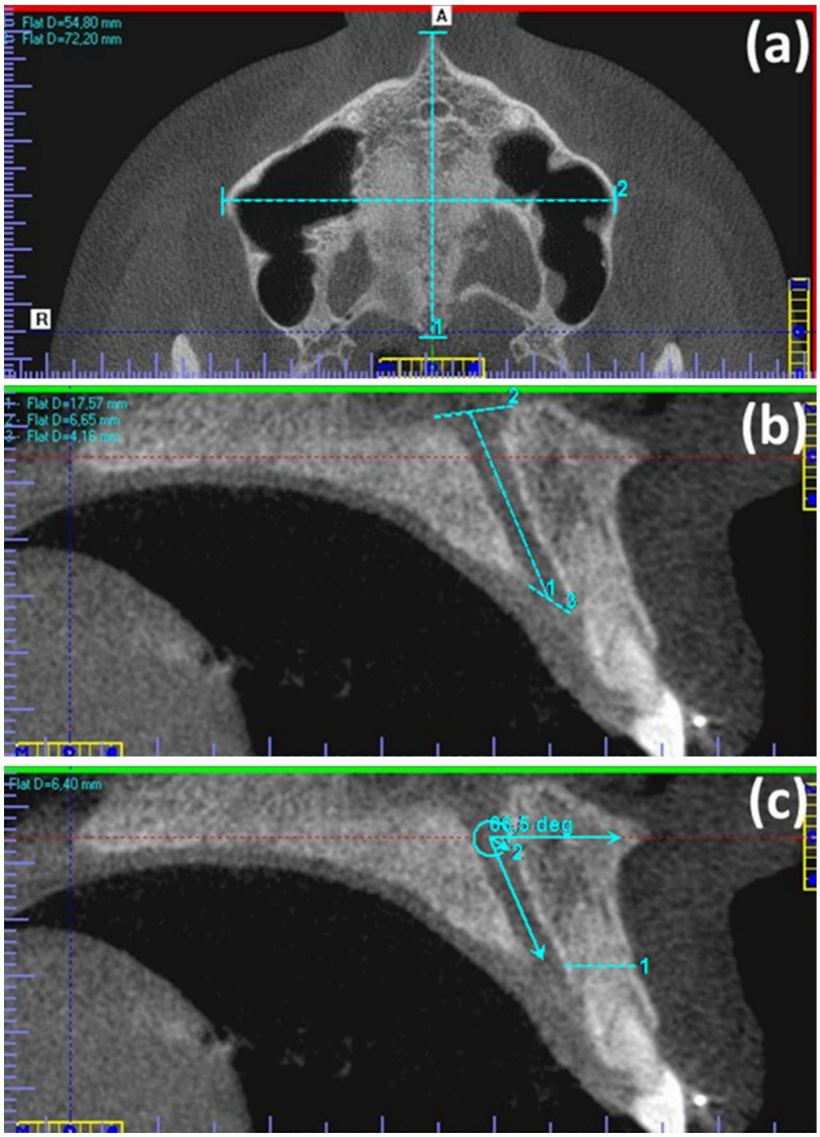

Figure 3. Representative CBCT scans of different sections of maxillary bone illustrating the way of measurement (green lines) of some variables as follows: (a) maximum MS height, (b) maximum MS depth, (c) maximum MS width; (d and e) minimum distance from the MS floor to the AC, (f) greater transverse width of IOF, (g) greater sagittal width of IOF, (h1) greater coronal width of IOF, (h2) distance from the mid-point of the IOF to the AC, (i) length of GPC in the sagittal plane, (j1) maximum anteroposterior width of the GPC in the axial plane, (j2) distance between GPC and pterygoid hamulus, (j3) distance between GPC and NPC, (j4) distance between GPC and PNS, (k1) distance from the center of GPF to the AC, (k2) distance between the medial wall of GPF and the midline maxillary suture, (l) angle formed by the horizontal plane of the palatine bone and the vertical axis of the GPC.

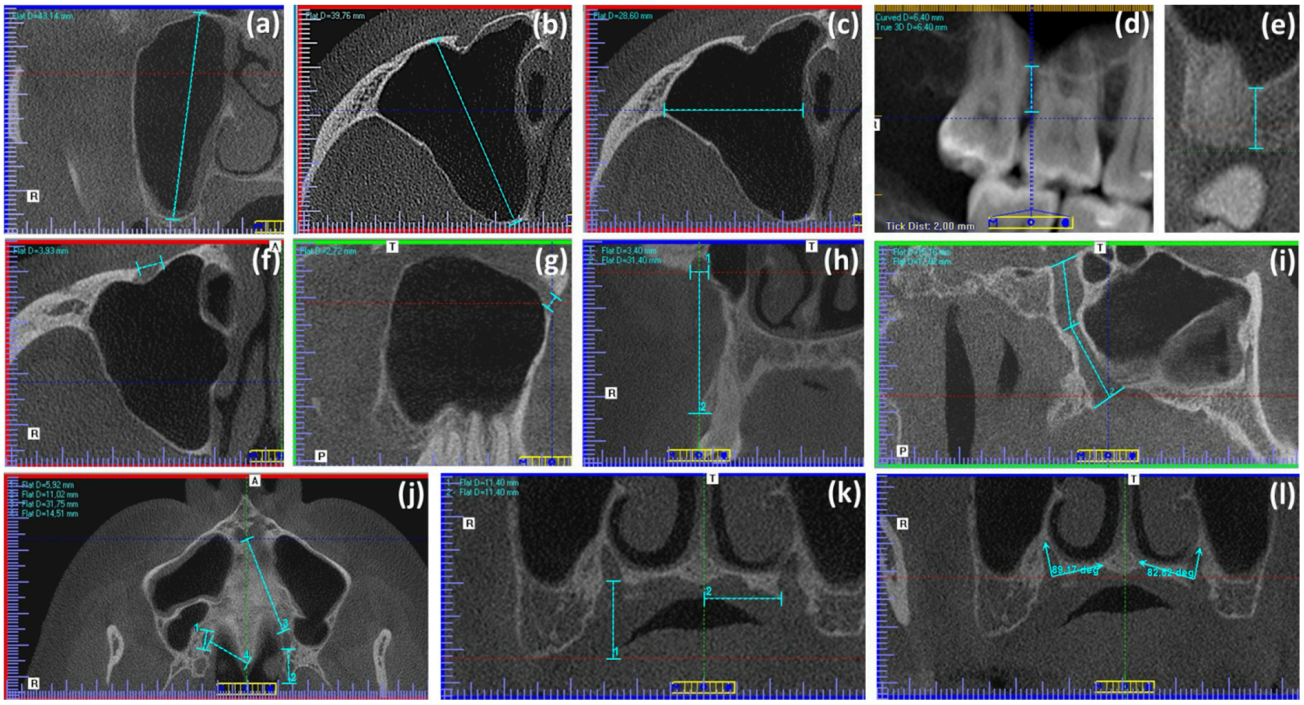

RESULTS

Study sample and reliability analysis:
Among DICOM files analyzed, 86 corresponded to males with an age range from 18 to 87 years (mean 46.99 ± 15.86) and 126 to females with an age range from 18 to 69 years (mean 50.46 ± 12.97). For each DICOM file, regardless of the sex, age, and alveolar process status, seven non-bilateral and 16 bilateral parameters were measured. The anterior maxillary alveolar process status was categorized as completely edentulous in 23 (10.80%) out of 212 cases, partially edentulous in 46 (21.70%) cases, and dentate in 143 (67.50%) cases. Likewise, 50 (11.8%) out of 424 posterior maxillary segments were classified as completely edentulous, 136 (32.10%) as partially edentulous, and 238 (56.10%) as dentate. No significant differences could be established for age and anterior/posterior alveolar process status with respect to sex nor for posterior alveolar process status between the left and right sides (all P-values >0.05, unpaired t or $\chi 2$ tests, data not shown), indicating an optimal comparability of data between the sexes in terms of age and alveolar process status. Likewise, there were no significant differences for bilateral measurements between maxillary sides (all P-values >0.05, unpaired t test, data not shown). The reproducibility analysis showed an excellent agreement among the two series of data obtained by the examiners for any of the quantitative parameters tested, with ICC values ranging between 0.893 and 0.999 (all P <0.001).

Between-group comparisons of tomographic measurements obtained from the sample
Tables 1 and 2 depict the bivariate comparisons of the non-bilateral or bilateral maxillary variables regarding to the sex distribution. From Table 1 can be seen that while no significant differences (all P >0.05 unpaired t test) were evidenced between sex categories regarding the NPC angle at sagittal plane and anteroposterior width of NPF, the mean values of the maxillary complex length, the maximum inter-maxillary width, the

length of NPC at sagittal plane, the minimum anterior-superior buccal bone thickness, and the anteroposterior width of IF were significantly higher in the male group (P <0.01) in comparison with those of the female group. In addition, Table 2 outlines how the dimensions related to the maximum height, depth, and width of MS; the axial, sagittal, and coronal measurements of IOF; the distance from the mid-point of IOF to the AC; length of GPC in the sagittal plane; the anteroposterior width of the GPC in the axial plane; the distance from the GPC to the pterygoid hamulus, NPC, and to PNS; along with the distance of GPF to the MMS and to AC were significantly higher (all P <0.05) in the male group in comparison with those calculated for the female group, whereas no significant differences (all P >0.05) were found among males and females in regards to the minimum distance from the sinus floor to the AC or the angle among the horizontal plane of PB and the GPC.

Table 1. Comparison of measurements related to specific non-bilateral maxillary variables with reference to the sex categories

Parameter[a]	Sex		*P*-value[b]
	Male (♂) (*n* = 86)	Female (♀) (*n* = 126)	
Maxillary complex length (mm)	53.81 ± 3.45	50.27 ± 3.14	<0.001
Maximum inter-maxillary width (mm)	67.67 ± 6.23	63.99 ± 5.51	<0.001
Length of NPC at sagittal plane (mm)	12.92 ± 2.72	11.08 ± 2.44	<0.001
NPC angle at sagittal plane (degrees)	69.48 ± 8.18	67.42 ± 9.58	0.104
Minimum anterosuperior buccal bone thickness (mm)	6.78 ± 1.68	5.91 ± 1.66	<0.001
Anteroposterior width of IF (mm)	3.92 ± 0.70	3.63 ± 0.85	0.009
Anteroposterior width of NPF (mm)	3.70 ± 1.85	3.45 ± 1.63	0.314

Abbreviations: NPC, nasopalatine canal; IF, incisive foramen; NPF, nasopalatine foramen

[a]Values are given as mean ± SD

[b]Two-sided unpaired *t*-test

Table 2. Comparison of measurements related to bilateral maxillary variables according to the sex category

Parameter[a,b]	Sex[a]		*P*-value[c]
	Male (♂) (*n* = 172)	Female (♀) (*n* = 252)	
Maximum maxillary sinus height (mm)	39.85 ± 3.87	35.27 ± 3.89	<0.001
Maximum maxillary sinus depth (mm)	37.59 ± 2.96	34.86 ± 3.10	<0.001
Maximum maxillary sinus width (mm)	28.98 ± 3.98	26.11 ± 4.21	<0.001
Minimum distance from the sinus floor to the AC (mm)	5.78 ± 3.44	6.08 ± 2.91	0.332
Greater width of IOF in the axial plane (mm)	4.70 ± 0.90	4.15 ± 0.94	<0.001
Greater width of IOF in the sagittal plane (mm)	4.14 ± 0.83	3.54 ± 0.87	<0.001
Greater width of IOF in the coronal plane (mm)	3.92 ± 0.68	3.56 ± 0.75	<0.001
Distance from the mid-point of the IOF to the AC (mm)	30.93 ± 2.95	29.73 ± 2.66	<0.001

Length of GPC in the sagittal plane (mm)	37.47 ± 3.17	35.11 ± 2.93	<0.001
Anteroposterior width of the GPC in the axial plane (mm)	6.28 ± 1.30	5.31 ± 1.27	<0.001
Distance from the GPC to the pterygoid hamulus (mm)	9.68 ± 1.45	8.93 ± 1.64	<0.001
Distance from the GPC to the NPC (mm)	33.20 ± 3.82	32.12 ± 3.00	0.001
Distance from the GPC to the PNS (mm)	15.97 ± 1.16	15.22 ± 1.28	<0.001
Distance from the medial wall of GPF to the MMS (mm)	13.77 ± 1.44	13.45 ± 1.38	0.021
Distance from the center of GPF to the AC (mm)	10.89 ± 2.30	9.45 ± 2.33	<0.001
Angle among the horizontal plane of PB and the GPC (degrees)	93.83 ± 8.02	93.82 ± 10.80	0.990

Abbreviations: AC, alveolar crest; IOF, infraorbital foramen; GPC, greater palatine canal; PNS, posterior nasal spine; NPC, nasopalatine canal; GPF, greater palatine foramen; MMS, midline maxillary suture; PB, palatine bone
[a]Data based on the sum of right- and left-maxillary posterior sides
[b]Values are given as mean ± SD
[c]Two-sided unpaired *t*-test

Findings from univariate and multivariate discriminant analysis.

To find the best axial, sagittal, and coronal maxillary predictors, all statistically significant variables identified in the bivariate analyses were included in univariate discriminant analyses, which are presented in Tables 3 and 4. From these tables is evident that Wilks' λ values varied from moderately high to very high in all of the constructs (0.748 to 0.987), thus indicating that there is considerable overlapping between the two groups. However, all χ^2 critical probability values were <0.05, demonstrating significant differences among men and women maxillary morphometric data. Furthermore, the results of the Box's M tests did not show statistically significant differences in the covariance matrices between sexes (all P >0.05) suggesting equality of covariance matrices between both groups. The univariate discriminant analysis of non-bilateral maxillary variables (Table 3) revealed a mean percentage of correct prediction after cross-validation ranging from 55.20% to 72.60%. The maxillary complex length showed the greatest accuracy (72.60%), and the anteroposterior width of IF exhibited the lowest value (55.20%). Similarly, the univariate discriminant analysis of bilateral maxillary variables (Table 4) showed mean percentages of correct prediction after cross-validation ranging from 58.70% to 73.10%. The maximum maxillary sinus height displayed the greatest accuracy (73.10%) whereas the distance from the medial wall of GPF to the MMS had the lowest value (58.70%). It is important to highlight that, cross-validation analysis demonstrated reduced accuracy percentages for 9 out of 19 variables included in the univariate discriminant analyses, while 10 variables showed the same mean correct prediction values, indicating that these methods produce acceptable results and are not overconfident. Considering that only the measurements obtained for maxillary complex length and maximum maxillary sinus height corresponded to average percentages above 70% in the univariate discriminant analyses, just the variables that presented correct prediction percentages above 60% were included in the multivariate discriminant analyses.

The results obtained from multivariate discriminant analysis of non-bilateral and bilateral maxillary variables for correct assignment by sex are presented in Tables 5 and 6, respectively. From these tables it can be seen the Fisher's linear discriminant function coefficients and the constants necessary to construct the discriminant equations, thus providing a direct method of classification for clinical application. It may be also noted in both predictive constructs that the Box's M covariance tests revealed equality between the matrices of male and female groups (P >0.05) thus suggesting a limited discrepancy in the predictor variables. Furthermore, Wilk's λ values decreased in the two multivariate models in comparison with those of the univariate counterparts, indicating that the groups of predictor measurements allow making statistically significant predictions in their outcomes (P <0.05). Moreover, the eigenvalues were far from zero and the canonical correlation

were moderate, so it is possible to assume that the variables used in each of the constructs led a moderately accurate distinction between the male and female groups. It was also noteworthy that the association of the variables in the multivariate models increased the percentages of correct sex prediction, even after cross-validation, up to 77.80% for non-bilateral and up to 77.40% for bilateral maxillary measurements.

Table 3. Univariate discriminant analysis and cross-validation for measurements related to specific non-bilateral maxillary variables

Parameter	Wilks' λ		Box's M		Correct prediction % ♂	Correct prediction % after cross-validation ♂	Correct prediction % ♀	Correct prediction % after cross-validation ♀	Mean correct prediction %	Mean correct prediction % after cross-validation
	Value	Significance	Value	Significance						
Maxillary complex length	0.778	<0.001	0.890	0.347	54.70	52.30	86.50	86.50	73.60	72.60
Maximum inter-maxillary width	0.911	<0.001	1.556	0.213	36.00	36.00	84.90	84.90	65.10	65.10
Length of NPC at sagittal plane	0.888	<0.001	1.133	0.288	44.20	44.20	83.30	82.50	67.50	67.00
Minimum anterior-superior buccal bone thickness	0.939	<0.001	0.016	0.898	33.70	33.70	84.10	84.10	63.70	63.70
Anteroposterior width of IF	0.968	0.009	3.660	0.056	18.60	16.30	81.70	81.70	56.10	55.20

Abbreviations: NPC, nasopalatine canal; IF, incisive foramen

Table 4. Univariate discriminant analysis and cross-validation for measurements related to bilateral maxillary variables

Parameter	Wilks' λ		Box's M		Correct prediction % ♂	Correct prediction % after cross-validation ♂	Correct prediction % ♀	Correct prediction % after cross-validation ♀	Mean correct prediction %	Mean correct prediction % after cross-validation
	Value	Significance	Value	Significance						
Maximum maxillary sinus height	0.748	<0.001	0.007	0.934	60.50	60.50	81.70	81.70	73.10	73.10
Maximum maxillary sinus depth	0.837	<0.001	0.450	0.503	49.40	49.40	81.30	81.30	68.40	68.40
Maximum maxillary sinus width	0.895	<0.001	0.633	0.427	44.20	44.20	80.60	79.80	65.80	65.30
Greater diameter of IOF at axial plane	0.920	<0.001	0.336	0.563	32.60	32.60	80.60	80.60	61.10	61.10
Greater diameter of IOF at sagittal plane	0.894	<0.001	0.527	0.468	39.00	39.00	82.10	81.30	64.60	64.20

Greater diameter of IOF at coronal plane	0.945	<0.001	1.480	0.224	25.00	25.00	83.30	83.30	59.70	59.70
Distance from the mid-point of the IOF to the AC	0.956	<0.001	2.239	0.135	27.30	27.30	88.10	88.10	63.40	63.40
Length of GPC at sagittal plane	0.872	<0.001	1.269	0.261	41.90	41.90	82.10	82.10	65.80	65.80
Anteroposterior diameter of the GPC at axial plane	0.878	<0.001	0.067	0.796	38.40	38.40	81.00	81.00	63.70	63.70
Distance from the GPC to the pterygoid hamulus	0.948	<0.001	2.883	0.090	24.40	24.40	82.90	82.50	59.20	59.00
Distance from the GPC to the NPC	0.973	0.001	2.984	0.084	19.80	19.20	91.30	90.90	62.30	61.80
Distance from the GPC to the PNS	0.918	<0.001	2.218	0.137	34.90	34.90	79.80	79.80	61.60	61.60
Distance from the medial wall of GPF to the MMS	0.987	0.021	0.468	0.495	7.00	4.70	95.60	95.60	59.70	58.70
Distance from the center of GPF to the AC	0.915	<0.001	0.027	0.871	34.90	34.90	85.30	83.70	64.90	63.90

Abbreviations: IOF, infraorbital foramen; AC, alveolar crest; GPC, greater palatine canal; PNS, posterior nasal spine; NPC, nasopalatine canal; GPF, greater palatine foramen; MMS, midline maxillary suture

Table 5. Multivariate discriminant analysis of measurements related to specific non-bilateral maxillary variables for correct assignment by sex

Measurements, Fisher's linear discriminant function coefficients, and equations	**Fisher Coefficient ♂**	**Fisher Coefficient ♀**	**Canonical discriminant functions and classification results**
Maxillary complex length	4.707	4.401	*n* = 212
Maximum inter-maxillary width	1.600	1.533	Box's M value = 7.651; significance = 0.679
Length of NPC at sagittal plane	1.382	1.130	Wilks' λ = 0.680; significance = <0.001
Minimum anterior-superior buccal bone thickness	0.337	0.170	Eigenvalue = 0.471; canonical correlation = 0.566
Constant	-191.746	-166.948	Correct prediction % ♂ = 67.40
Equations ♂ = 4.707*Maxillary complex length + 1.600*Maximum maxillary transverse width + 1.382*Length of NPC at sagittal plane + 0.337*Minimum anterior-superior buccal bone thickness – 191.746 ♀ = 4.401*Maxillary complex length + 1.533*Maximum maxillary transverse width + 1.130*Length of NPC at sagittal plane + 0.170*Minimum anterior-superior buccal bone thickness – 166.948			Correct prediction % after cross-validation ♂ = 66.30 Correct prediction % ♀ = 87.30 Correct prediction % after cross-validation ♀ = 85.70 Mean correct prediction % = 79.20 Mean correct prediction % after cross-validation = 77.80

Abbreviations: NPC, nasopalatine canal; IF, incisive foramen

Table 6. Multivariate discriminant analysis of measurements related to bilateral maxillary variables for correct assignment by sex regardless of the side

Measurements, Fisher's linear discriminant function coefficients, and equations	Fisher Coefficient ♂	Fisher Coefficient ♀	Canonical discriminant functions and classification results
Maximum maxillary sinus height	0.358	0.179	*n* = 424
Maximum maxillary sinus depth	2.354	2.258	Box's M value = 84.401; significance = 0.089
Maximum maxillary sinus width	-0.330	-0.356	Wilks' λ = 0.605; significance = <0.001
Greater diameter of IOF at axial plane	2.812	2.454	Eigenvalue = 0.652; canonical correlation = 0.628
Greater diameter of IOF at sagittal plane	-0.668	-0.971	Correct prediction % ♂ = 69.20
Distance from the mid-point of the IOF to the AC	3.243	3.231	Correct prediction % after cross-validation ♂ = 68.00
Length of GPC at sagittal plane	2.176	2.123	Correct prediction % ♀ = 84.10
Anteroposterior diameter of the GPC at axial plane	3.728	3.259	Correct prediction % after cross-validation ♀ = 83.70
Distance from the GPC to the NPC	2.466	2.407	Mean correct prediction % = 78.10
Distance from the GPC to the PNS	9.498	9.039	Mean correct prediction % after cross-validation = 77.40
Distance from the center of GPF to the AC	-0.324	-0.429	
Constant	-270.389	-241.129	

Equations:

♂ = 0.358*Maximum maxillary sinus height + 2.354*Maximum maxillary sinus depth - 0.330*Maximum maxillary sinus width + 2.812*Greater diameter of IOF in the axial plane - 0.668*Greater diameter of IOF in the sagittal plane + 3.243*Distance from the mid-point of the IOF to the AC + 2.176*Length of GPC in the sagittal plane + 3.728*Anteroposterior diameter of the GPC in the axial plane + 2.466*Distance from the GPC to the NPC + 9.498*Distance from the GPC to the PNS - 0.324*Distance from the center of GPF to the AC - 270.389

♀ = 0.179*Maximum maxillary sinus height + 2.258*Maximum maxillary sinus depth - -0.356*Maximum maxillary sinus width + 2.454*Greater diameter of IOF in the axial plane - 0.971*Greater diameter of IOF in the sagittal plane + 3.231*Distance from the mid-point of the IOF to the AC + 2.123*Length of GPC in the sagittal plane + 3.259*Anteroposterior diameter of the GPC in the axial plane + 2.407*Distance from the GPC to the NP+ 9.039*Distance from the GPC to the PNS - 0.429*Distance from the center of GPF to the AC – 241.129

Abbreviations: IOF, infraorbital foramen; AC, alveolar crest; GPC, greater palatine canal; PNS, posterior nasal spine; NPC, nasopalatine canal; GPF, greater palatine foramen; MMS, midline maxillary sutur

DISCUSSION

It is accepted that skeletal sex estimation in unknown human remains is based on the sexually dimorphic expression of bony features that occur through different patterns, rates and growth periods.[26] Given that mandible and maxilla exhibit different morphological variations between males and females,[6,27-29] these bones may be suitable for sex estimation. However, although compelling evidence concerning sexual dimorphism has emphasized the need for determining anthropometric standards for

different populations,[2,6,8,10] to the best of the authors knowledge, this is the first study to demonstrate sex dimorphism of adult humans based on the discriminant function analysis of morphometric parameters of various maxillary structures analyzed using CBCT scans. In a previous study, the authors demonstrated, using similar imaging methods that maxillary bone can present several dimensional differences that may be strongly liaised to sex, but are independent of age, side, and of the alveolar process status[13]. In the present study, the authors used a different method to compare the maxillary dimensions with the majority of the DICOM files previously analyzed, but excluding of all cases with outlier data,[30] and including new DICOM files in order to uphold the estimates at an optimal level of accuracy against the effect of decreased sample size caused by the exclusions. It is worth noting that intra-observer repeatability was significantly excellent for the measurements evaluated in all multiplanar reconstructions, so this study supports the view that CBCT imaging constitutes a simple, reliable, and valid technique for the assessment of morphometric characteristics of the maxillary bone.

The bivariate analyses of this study demonstrated higher mean values for several non-bilateral and bilateral maxillary measurements in males compared to female data, with the exception of the NPC angle at sagittal plane, the anteroposterior width of NPF, the minimum distance from the sinus floor to the AC, and the angle between the horizontal plane of PB and the GPC. Among the analyzed variables, 7 out of 9 (77.77%) non-bilateral and 14 out of 16 (87.5%) bilateral maxillary parameters showed sexual dimorphism. Altogether, these results confirm previous findings demonstrating that maxillary bone can present multiple morphological and dimensional differences toughly liaised to sex.[7,8,12,13,23,27] Alternatively, the present findings might parallel, at least partially, those of previous anthropometric studies that have applied diverse statistical protocols for sex prediction from cranial metric traits using limiting points, sectioning points, demarking points, logistic regression analysis, discriminant function analysis, support vector machine modeling, machine learning algorithms, and deep learning artificial neural network models.[5,31-35] Although the exact explanation for sex differences has not been fully clarified, it has been argued that these variations might be caused by several factors influencing the bone remodelling process including genetic background, ethnicity, sex hormone actions, muscle mass, masticatory muscle activities, and socio-economy environment.[27]

Discriminant function analysis has become a broadly used and accepted approach for sex estimation from human skeletal remains. In the current study, several univariate discriminant analyses were conducted to evaluate the usefulness of individual predictor variables to discriminate the sexes from each other. It should be noted that this stage focused on the inclusion of variables that showed significant differences in the bivariate comparisons, while non-significant variables were excluded due to the lack of discriminatory capacity. For the included variables, Wilks' λ values ranged from 0.987 to 0.748 across the analyses, representing a range from 1.3% to 25.2% of variance explained. Given that all χ^2 critical probability values were <0.05, these results suggest that, when considered individually, all morphometric variables included in the analyses contributed to the sex group separation. Among these variables, both the maxillary complex length linked to specific non-bilateral maxillary variables (mean correct prediction % after cross-validation = 72.60%) and the maximum maxillary sinus height linked to bilateral maxillary variables (mean correct prediction % after cross-validation = 73.10%) presented the greatest sexual dimorphism confirming the results of other researchers.[7,8] Notwithstanding the aforementioned, just the variables showing correct prediction percentages above 60% were merged in the multivariate analyses.

The stepwise multivariate discriminant function analysis was conducted to determine the optimal combination of variables for discriminant functions and their weighting to reflect the contribution to sex estimation.[1] It is important to point out that, in agreeance with previous results,[10] although Wilks' λ values revealed a low discriminant power of the variables included in the constructs, their values improved as more variables were included in each discriminant model. In consonance with the former, it has been recognized that the increasing number of variables might affect the results and enhance the accuracy of measurements.[36] The discriminant functions obtained from this study were tested

for accuracy using leave-one-out cross-validation methods to evaluate such classifications.[5] It has been accepted that, since sex constitutes a discrete dichotomous variable, the probability of correctly estimating the sex at random would be 50%.[10] In the present study using a series of maxillary bone measurements, the mean correct percentage reached after cross-validation to estimate sex was statistically significant and 27.40% to 27.80% higher using either bilateral or non-bilateral maxillary variables than that yielded at random, thus suggesting a good level of sex identification. Moreover, in view of that sex may be determined from the complete skull with 80% accuracy,[37] the findings herein presented indicate that maxillary bone is a reliable sex predictor.

Finally, several limitations were identified in this study. First, acquisition of CBCT images was based on parameters used for live adult individuals, so these could be adapted to preserve the image quality and make the measurements reproducible in case of evaluating deceased individuals and bone remnants.[8] Second, Colombian population possesses a heterogeneous ethnographic profile. This circumstance may impede the generalizability of the findings to other ethnic groups with dissimilar maxillary morphological characteristics.[13] Consequently, it is necessary to design discriminant functions for different populations in order to evaluate the effectiveness of this sex identification method. Third, considering that some researchers argue that sexual dimorphism is not manifest at an appreciable level until after pubertal modifications have taken place,[38,39] mainly due to the different growth and development patterns between males and females,[27] the functions presented can be applied to maxillary bones of adult individuals but have limited value before puberty. Hence, additional studies using different approaches, such as discriminant analyses based on permanent tooth dimensions, are required for subadult sex estimation. Fourth, although the increased values of 19 variables were significantly associated with the male sex in the bivariate comparisons, additional factors, comprising age, extent of tooth loss, and wearing prosthesis might have an important influence on the reported data. Nevertheless, according to the findings presented, it seems that, irrespective of age, dental, and prosthetic conditions, all of these parameters are robustly liaised to the male sex.

CONCLUSION

Within the limitations of the study, it can be concluded that, CBCT measurement of maxillary bone parameters may be applied as a complementary technique to discriminate the sex from human remains through discriminant function analysis methods in the Colombian population.

ACKNOWLEDGMENT

The authors thank RADEX 3D Specialized Radiology Center for providing CBCT images and its software for the study purpose.

REFERENCES

1. Anuthama K, Shankar S, Ilayaraja V, Kumar GS, Rajmohan M, Vignesh. Determining dental sex dimorphism in South Indians using discriminant function analysis. Forensic Sci Int. 2011:212:86-9.
2. Partido Navadijo M, Monge Calleja ÁM, Ferreira MT, Alemán Aguilera I. Validation of discriminant functions from the rib necks in two Portuguese adult identified populations. Int J Legal Med. 2023;137:851-61.
3. Audenaert EA, Pattyn C, Steenackers G, De Roeck J, Vandermeulen D, Claes P. Statistical shape modeling of skeletal anatomy for sex discrimination: their training size, sexual dimorphism, and asymmetry. Front Bioeng Biotechnol. 2019;7:302.
4. Litsas G. Growth hormone and craniofacial tissues. An update. Open Dent J. 2015;9:1-8.
5. Krishan K, Chatterjee PM, Kanchan T, Kaur S, Baryah N, Singh RK. A review of sex estimation techniques during examination of skeletal remains in forensic anthropology casework. Forensic Sci Int. 2016;261:165.e1-8.
6. Lopez-Capp TT, Rynn C, Wilkinson C, de Paiva LAS, Michel-Crosato E, Biazevic MGH. Discriminant analysis of mandibular measurements for the estimation of sex in a modern Brazilian sample. Int J Legal Med. 2018;132:843-51.
7. Paknahad M, Shahidi S, Zarei Z. Sexual dimorphism of maxillary sinus dimensions using cone-beam computed tomography. J Forensic Sci. 2017;62:395-8.
8. Farias Gomes A, de Oliveira Gamba T, Yamasaki MC, Groppo FC, Haiter Neto F, Possobon RF. Development and validation of a formula based on maxillary sinus measurements as a tool for sex estimation: a cone beam computed tomography study. Int J Legal Med. 2019;133:1241-9.
9. Fortes de Oliveira O, Lima Ribeiro Tinoco R, Daruge Júnior E, Silveira Dias Terada AS, Alves da Silva RH, Paranhos LR. Sexual dimorphism in Brazilian human skulls: discriminant function analysis. J Forensic Odontostomatol. 2012;30:26-33.
10. Lopez-Capp TT, Rynn C, Wilkinson C, Paiva LAS, Michel-Crosato E, Biazevic MGH. Sexing the cranium

from the foramen magnum using discriminant analysis in a Brazilian sample. Braz Dent J. 2018;29:592-8.
11. Gibelli D, Borlando A, Dolci C, Pucciarelli V, Cattaneo C, Sforza C. Anatomical characteristics of greater palatine foramen: a novel point of view. Surg Radiol Anat. 2017;39:1359-68.
12. Görürgöz C, Öztaş B. Anatomic characteristics and dimensions of the nasopalatine canal: a radiographic study using cone-beam computed tomography. Folia Morphol (Warsz). 2021;80:923-34.
13. Palacio-Gutiérrez S, Morales-Galeano S, Obando-Castillo JL, Saldarriaga-Naranjo CI, Tobón-Arroyave SI. Logistic regression analysis of sex-related morphological and dimensional variations of maxillary bone: a cone-beam computed tomography-based retrospective study. Eur J Anat. 2023;27:741-58.
14. Manzanera E, Llorca P, Manzanera D, García-Sanz V, Sada V, Paredes-Gallardo V. Anatomical study of the maxillary tuberosity using cone beam computed tomography. Oral Radiol. 2018;34:56-65.
15. Bahşi İ, Orhan M, Kervancıoğlu P, Yalçın ED. Morphometric evaluation and clinical implications of the greater palatine foramen, greater palatine canal and pterygopalatine fossa on CBCT images and review of literature. Surg Radiol Anat. 2019;41:551-67.
16. Bahşi I, Orhan M, Kervancıoğlu P, Yalçın ED, Aktan AM. Anatomical evaluation of nasopalatine canal on cone beam computed tomography images. Folia Morphol (Warsz). 2019;78:153-62.
17. Jayasinghe RM, Hettiarachchi PVKS, Fonseka MCN, Nanayakkara D, Jayasighe RD. Morphometric analysis of nasopalatine foramen in Sri Lankan population using CBCT. J Oral Biol Craniofac Res. 2020;10:238-40.
18. Glowacki J, Christoph K. Gender differences in the growing, abnormal, and aging jaw. Dent Clin North Am. 2013;7:263-80.
19. Kotsiomiti E, Farmakis N, Kapari D. Factors related to the resting tongue position among partially and completely edentulous subjects. J Oral Rehabil. 2005;32:397-402.
20. Nanayakkara D, Peiris R, Mannapperuma N, Vadysinghe A. Morphometric analysis of the infraorbital foramen: the clinical relevance. Anat Res Int. 2016;2016:7917343.
21. Dagistan S, Miloğlu Ö, Altun O, Umar EK. Retrospective morphometric analysis of the infraorbital foramen with cone beam computed tomography. Niger J Clin Pract. 2017;20:1053-64.
22. Tomaszewska IM, Kmiotek EK, Pena IZ, Średniawa M, Czyżowska K, Chrzan R, et al. Computed tomography morphometric analysis of the greater palatine canal: a study of 1,500 head CT scans and a systematic review of literature. Anat Sci Int. 2015;90:287-97.
23. Rapado-González O, Suárez-Quintanilla JA, Otero-Cepeda XL, Fernández-Alonso A, Suárez-Cunqueiro MM. Morphometric study of the greater palatine canal: cone-beam computed tomography. Surg Radiol Anat. 2015;37:1217-24.
24. Ikuta CR, Cardoso CL, Ferreira-Júnior O, Lauris JR, Souza PH, Rubira-Bullen IR. Position of the greater palatine foramen: an anatomical study through cone beam computed tomography images. Surg Radiol Anat. 2013;35:837-42.
25. Cicchetti DV. Guidelines, criteria, and rules of thumb for evaluating normed and standardized assessment instruments in psychology. Psychol Assess. 1994;6:284–90.
26. Raghavendra Babu YP, Kanchan T, Attiku Y, Dixit PN, Kotian MS. Sex estimation from foramen magnum dimensions in an Indian population. J Forensic Leg Med. 2012;19:162-7.
27. Astuti ER, Iskandar HB, Nasutianto H, Pramatika B, Saputra D, Putra RH. Radiomorphometric of the jaw for gender prediction: a digital panoramic study. Acta Med Philipp. 2022;56:113-21.
28. Senol GB, Tuncer MK, Nalcaci N, Aydin KC. Role of mandibular anatomical structures in sexual dimorphism in Turkish population: a radiomorphometric CBCT study. J Forensic Odontostomatol. 2022;40:53-64.
29. Munhoz L, Okada S, Hisatomi M, Yanagi Y, Arita ES, Asaumi J. Are computed tomography images of the mandible useful in age and sex determination? A forensic science meta-analysis. J Forensic Odontostomatol. 2024;42:38-57.
30. Stella O. Discriminant analysis: an analysis of its predictship function. J Educ Pract. 2019;10:50-7.
31. Del Bove A, Veneziano A. A generalised neural network model to estimate sex from cranial metric traits: A robust training and testing approach. Appl Sci. 2022;12:9285.
32. Toy S, Secgin Y, Oner Z, Turan MK, Oner S, Senol D. A study on sex estimation by using machine learning algorithms with parameters obtained from computerized tomography images of the cranium. Sci Rep. 2022;12:4278.
33. Bertsatos A, Chovalopoulou ME, Brůžek J, Bejdová Š. Advanced procedures for skull sex estimation using sexually dimorphic morphometric features. Int J Legal Med. 2020;134:1927-37.
34. Bewes J, Low A, Morphett A, Pate FD, Henneberg M. Artificial intelligence for sex determination of skeletal remains: Application of a deep learning artificial neural network to human skulls. J Forensic Leg Med. 2019;62:40-43.
35. Franklin D, Cardini A, Flavel A, Kuliukas A. Estimation of sex from cranial measurements in a Western Australian population. Forensic Sci Int. 2013;229:158.e1-8.
36. Fernandes CL. Forensic ethnic identification of crania: the role of the maxillary sinus--a new approach. Am J Forensic Med Pathol. 2004;25:302-13.
37. Saukko P, Knight B. Knight's forensic pathology. Boca Raton: CRC Press; 2016.
38. Scheuer L. A blind test of mandibular morphology for sexing mandibles in the first few years of life. Am J Phys Anthropol. 2002;119:189-91.
39. Franklin D, Oxnard CE, O'Higgins P, Dadour I. Sexual dimorphism in the subadult mandible: quantification using geometric morphometrics. J Forensic Sci. 2007;52:6-10.